Egypt. J. Chem. **Vol. 62**, No. 4 pp. 573 - 581 (2019)

Egyptian Journal of Chemistry

http://ejchem.journals.ekb.eg/

Green Synthesis and Characterization of Yttrium Oxide, Copper Oxide and Barium Carbonate Nanoparticles Using *Azadirachta Indica* (the Neem Tree) Fruit Aqueous Extract

Imad Hamadneh[1*], Hadeel Alhayek[1], Ahmed Al-Mobydeen[1], Afnan Abu Jaber[1], Rula Albuqain[2], Shorouq Alsotari[2], Ammar Al-Dujaili[3]

[1]*Chemistry Department, Faculty of Science, University of Jordan, 11942 Amman, Jordan.*

[2]*Cell Therapy Center (CTC), University of Jordan, 11942 Amman, Jordan.*

[3]*Hamdi Mango Center for Scientific Research, University of Jordan, 11942 Amman, Jordan.*

GREEN chemistry was used to prepare yttrium oxide (Y_2O_3), barium carbonate ($BaCO_3$), and copper oxide (CuO) nano-particles (NPs) using aqueous Neem fruit extract *Azadirachta indica* as a capping agent. The resulted metal complexs were calcined at temperature of 750°C. The produced NPs were characterized using X-ray Powder Diffraction (XRD), Scanning and Transmission Electron Microscope (STEM), Fourier transform infrared spectroscopy (FTIR), UV-Vis Spectroscopy and Thermal Gravimetric Analysis (TGA). XRD analysis confirmed the monoclinic structure for CuO NPs, orthorhombic structure for $BaCO_3$ NPs and cubic structures for Y_2O_3 NPs. XRD data for the three metal oxides were matched with the ICDD standards. The crystallite size for the CuO, $BaCO_3$ and Y_2O_3 NPs were 29.9, 49.0 and 10.3 nm, respectively. UV-vis spectroscopy showed that for the scanned suspended oxides were in the UV range which is an indication of the formation of nano-sized materials. STEM results showed agglomerated NPs with an average particle size of < 50 nm for all oxide samples. FTIR results confirmed that the metal-oxide bond existed and represented by bands in the range 500-700 nm^{-1}.

Keywords: Metal complex, Metal oxides NPs, Neem fruit extract, Green chemistry, Calcination.

Introduction

Synthesis of Nanoparticle (NPs) has gained an emerging interest as a result of their superior properties and potential applications in almost every field such as catalysis [1,2], magnetic [3], antimicrobial activity [4], sensors and others. Moreover, thermal, catalytic and mechanical characteristics of a material are altered as surface to volume ratio increases [1,5]. Using chemical methods for the preparation of NPs are toxic and expensive, and the by-products have negative impact on the environment. Therefore, green techniques became the best alternative [6].

A considerable attention has been directed towards using plant materials to synthesize metallic and metallic oxide NPs in an eco-friendly (green) approach by employing several organisms (fungi, yeast, bacteria, plants and macro and micro-nutrients such as proteins, peptides, vitamins and reducing sugars) has gained a great attention [7,8, 9]. Plant-based synthesis of NPs has mainly focused on precious metals (gold and silver) and the synthesized NPs by the green method exhibit a wide range of sizes and shapes comparable to those synthesized by other organisms [10]. Plant extracts can act both as reducing and capping agents in NPs synthesis [11]. Surface morphology and the size of metal NPs are highly influenced by the plant extract materials [12].

Azadirachta indica also known as Neem was used in medicine and medical applications throughout centuries in India, and different parts of Asia and Africa [13]. The leaves extract was

*Corresponding author e-mail: i.hamadneh@ju.edu.jo
Received 26/9/2018; Accepted 14/1/2019
DOI: 10.21608/ejchem.2018.5281.1469

used to synthesize copper and platinum NPs. The resulted NPs were highly crystalline with an average size of 5-48nm [14]. ZnO nanotubes were synthesized by leaf extract of *Azadirachta indica*. It shows highly crystalline with an average particle size of 25 nm [15]. Titanium NPs were synthesized from titanium isopropoxide using *Azadirachta indica* extract. The resulted NPs exhibited spherical shape with particle size ranging from 15-42 nm [16, 17]. In this work, Y_2O_3, $BaCO_3$ and CuO NPs were prepared by green method using *Azadirachta indica* fruit aqueous extract, the resulted NPs were characterized using FTIR, TGA, XRD, UV-visible spectroscopy, TEM and SEM.

Experimental

Preparation of Azadirachta indica extract

Neem fruits (*Azadirachta indica*) were washed with water several times, air-dried for 3weeks and then crushed into small pieces (< 0.5mm). An approximate weight of 50.0 g from crushed Neem was boiled in 500 mL of distilled water for 30 minutes and then cooled to room temperature. The physical appearance was monitored. The slurry was filtered using suction filtration and centrifugation at 6000 rpm for 10 min using Hermle Centrifuge Model Z200A. The extract was stored in dark at 4.0°C for further use.

Preparation of Y_2O_3, CuO and $BaCO_3$ NPs

A 50 mL of 0.10*M* metal acetate solution was titrated with 250 mL of neem extract for 10 minutes at 1000 rpm. The solution was kept in ultrasonic bath for 10 minutes at 30°C. The brown precipitate was filtered, dried overnight. Based on the TGA results the calcined temperature for all metal complexes is 750°C using a muffle furnace for 2 hours.

Characterizations

The resulted powders were characterized using Furrier Transform Infrared (FT-IR) technique using Thermo Nicolet Nexus 670 FTIR spectrophotometer equipped with attenuated total reflection (ATR) sampling accessory. Thermo Gravimetric Analysis (TGA) using a Netzsch STA 409 PG/PC thermal analyzer (Selb Bavaria, Germany) was used for weight loss determination. X-ray powder diffraction (XRD) (7000 Shimadzu with Cu K_a 1.5418Å was used for phase identification and Check Cell free-software was used for analysis. Dual Beam Field Emission Scanning Electron Microscope model FEI, Versa 3D with STEM attachment was used for morphological studies. Dual beam UV-VIS spectrophotometer Model Cary 100, Varian-Bio was used for measuring the Lambda max for all nonmaterials.

Results and Discussion

Figure 1 showed the weight loss for all complexes at function of temperature, TGA showed a sharp weight loss between 150-550°C due to the removal of adsorbed water on the surface of the complexes, water of crystallization and the decomposition of organic constituents. The formation of Y_2O_3 and CuO was above 550°C

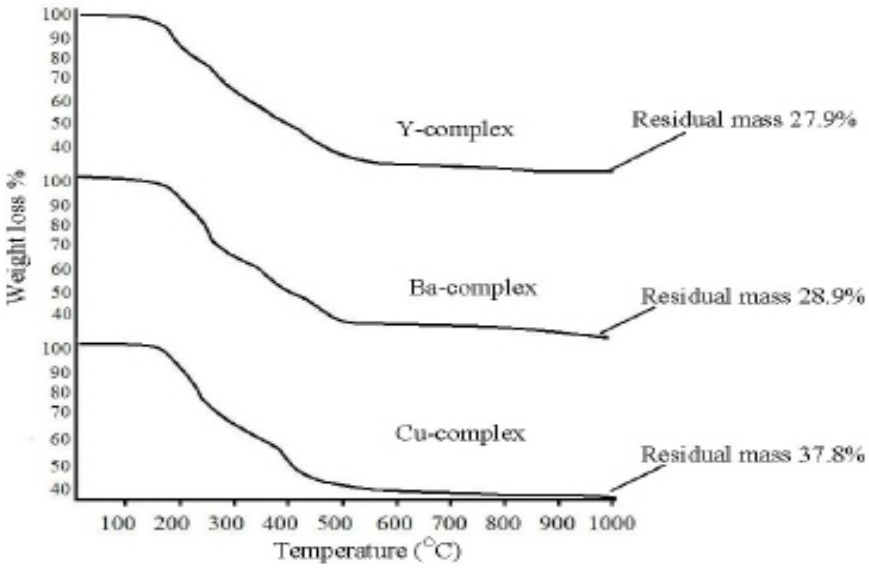

Fig. 1. Thermal gravimetric analysis (TGA) curve of dried metal-complexes.

mean while the formation of BaO was above 800°C.

The X-ray pattern for yttrium complex (Fig. 2a) showed an amorphous structure with a broad peak at 21°, 28° and 43° Barium complex in Fig. 2b showed an amorphous structure with broad peak at 2=35°. Copper complex in Fig. 2c showed an amorphous structure with broad peak at 2 = 19°, 36.5° 42.9°, 43.7°, 51°, 61.7° and 74°. Figure 3a showed the calcined Y_2O_3 NPs, high intensity peaks at 20.9 °, 24.4 °, 29.8 °, 32.4°, 36.8°, 40.8°, 44.5°, 57.5°, 60.5°, 64.9°, 71.6° and 77.1° are belonging to cubic structure with space group of Ia3, the lattice parameter (a_o) is 10.37Å +0.01 where, and are 90.00° . This result is matched with the reference (ICDD# 00-001-0831).

The calcined NPs for $BaCO_3$ are shown in Fig. 3b, the XRD analysis showed that all identified peaks at 24.2 °, 24.6 °, 27.2 °, 29.2 °, 30.4 °, 42.3 °, 39.8 °, 42.3 °, 44.6 °, 45.2 °, 46.9 °, 53.8 °, 60.2 °, 61.4 °, 70.1 °, 71.9 °, 75.7 °, 77.5 ° and 87.2 ° are belonging to Orthorhombic structure with space group of P/mmm, the lattice parameter a_o, b_o and c_o are 6.25 Å, 8.83 Å and 6.55 Å with precision of +0.01, where, and are 90.00° and it was matched with reference (ICDD# 00-002-0364). Figure 3c showed the calcined NPs for CuO, all the identified peaks 32.8 °, 35.9 °, 39.1°, 46.6°, 49.0°, 53.9°, 58.6°, 61.9°, 66.5°, 68.5°, 72.7°, 75.6°, 80.5 and 83.7° are belonging to monoclinic structure with space group of C2/c, the lattice parameters a_o, b_o and c_o are 4.68 Å, 3.40 Å and 5.10 Å with precision of +0.01, where is 99.53°, and are 90.00°. The results are matched with reference (ICDD# 00-001-1117). The average crystallite size D_{hkl} for the resulted materials can be estimated using Scherrer equation (1) [18]:

$$D_{hkl} = k\lambda/\beta cos\theta \qquad (1)$$

where k is the shape factor (k=0.9), l is the wavelength of the radiation Cu = 1.5418 Å and is the full width at half maximum (FWHM) in radians. The crystalline sizes are 29.9 nm 0.1, 40.0 nm± 0.1 and 10.3 nm 0.1, for CuO, $BaCO_3$ and Y_2O_3, respectively.

The FT-IR spectrum metal-complex is shown in Fig. 4. The sharp bands appeared at 596 cm^{-1} and 1013 cm^{-1} are Corresponding to the existence of metal-complex, the C-H aldehyde stretching mode was found at the range 1251-1395 cm^{-1} and C=C stretching mode at 1396 -1461cm^{-1}. The bands appeared at 1567-1595 cm^{-1} and 1740-1743 cm^{-1} were assigned to the C=O carboxylic anion

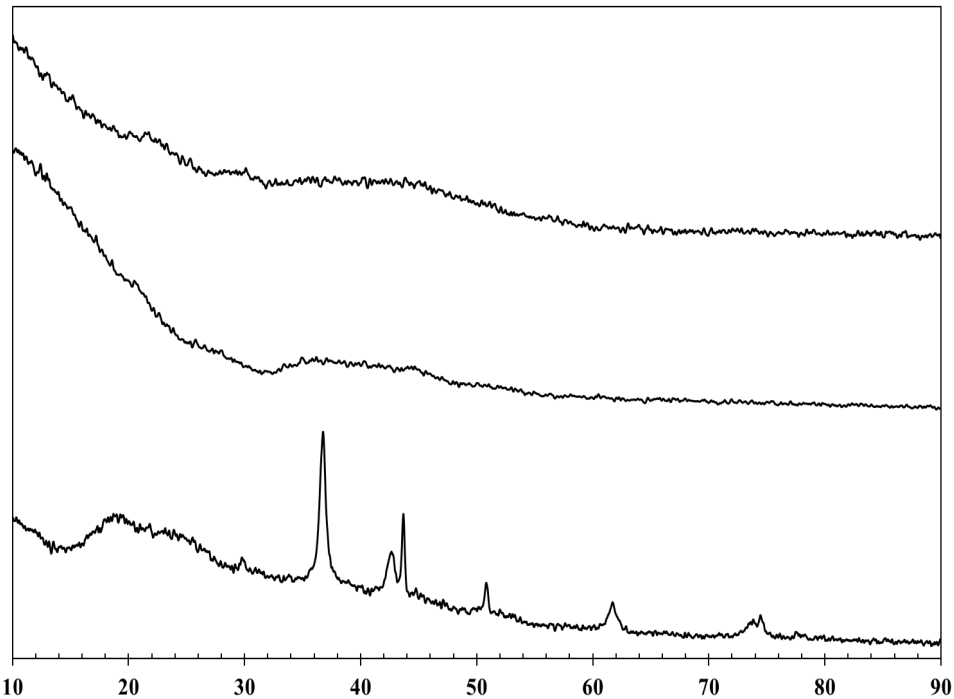

Fig. 2. XRD pattern for (a) Y-complex, (b) Ba-complex and (c) Cu-complex.

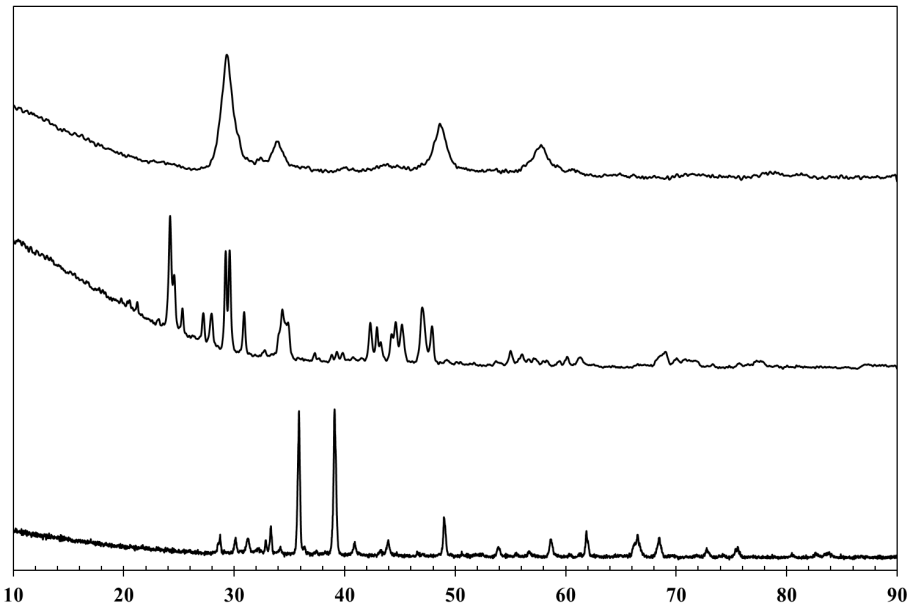

Fig. 3. XRD pattern for (a) Y_2O_3 NPs, (b) $BaCO_3$ NPs and (c) CuO NPs.

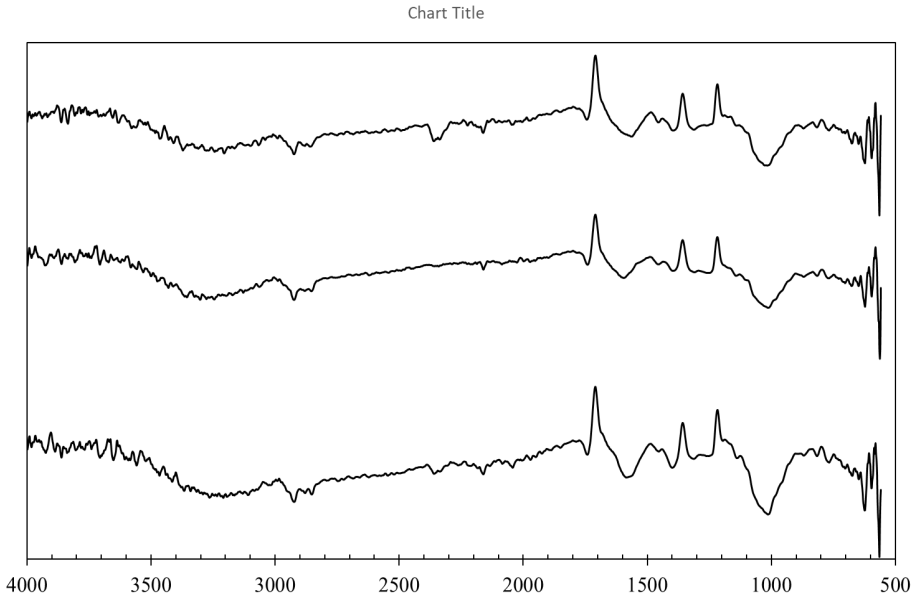

Fig. 4. The FT-IR spectrum before calcination (a) Y-complex, (b) Cu-complex and (c) Ba-complex.

and ketone stretching modes, respectively. The band located at 677 cm^{-1} for C-S sulfide stretching mode. The adsorbed CO_2 was found at 2160 cm^{-1}. Finally, the band at 2923 cm^{-1} was assigned to (O-H) of phenol group stretching mode.

The FT-IR spectrum of Y_2O_3 is shown in Fig. 5a, where a sharp peak appears at 565 cm^{-1} that assigned to (Y-O) stretching vibration and Y_2O_3 formation, the intense peak at 588 cm^{-1} corresponds to the anti-symmetric Y–O–Y stretching mode of the surface–bridging oxide. The peak at 873 cm^{-1} is responsible for the presence of trace of Y–OH. The peaks at 1216, 1085 and 1026 cm^{-1} are the characteristic asymmetric stretching of Y–O–Y present in the nanostructure [19].

The FT-IR spectrum CuO is shown in Fig.

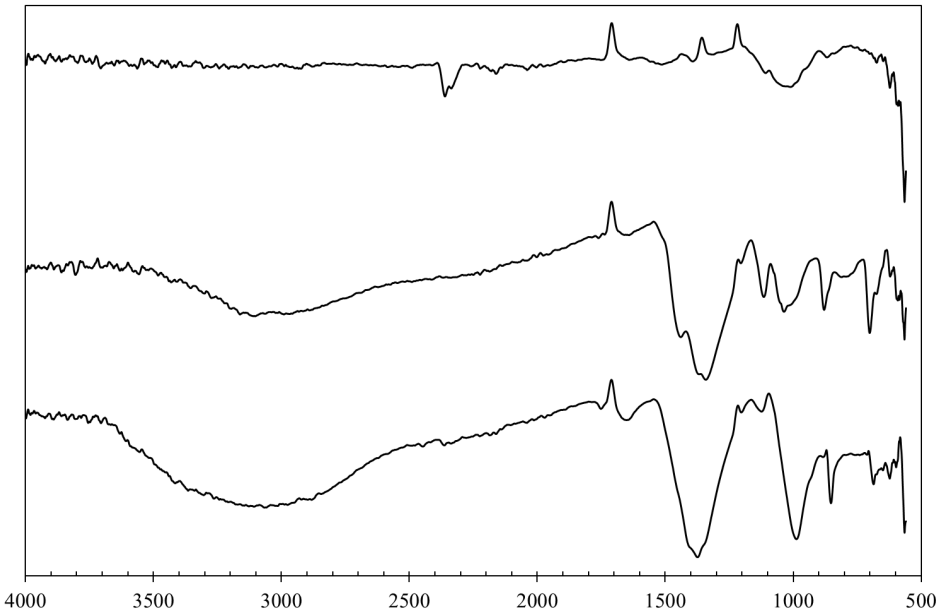

Fig. 5. FT-IR spectrum after calcination (a) Y_2O_3 NPs, (b) CuO NPs and (c) $BaCO_3$ NPs.

5b. A strong absorption bands located at 591 cm^{-1} and 701 cm^{-1} were assigned to the vibration of the Cu-O, the bands at 2382 cm^{-1} and 1660 cm^{-1} are corresponding to C-O stretching mode and C=O stretching mode, respectively. 1073 cm^{-1} peak corresponding to C-O, 1344 cm^{-1} Cu-O cm^{-1}, the band which represents the formation of covalent bond between OH on the surface of Cu (Cu-OH) was located at 1546 cm^{-1}. The broad band appeared between 2800-3100cm^{-1} is assigned to O-H stretching vibration caused by the presence of water molecules [20,21].

The FT-IR spectrum for $BaCO_3$ is shown in Fig. 5c, the vibration frequency at 565 cm^{-1} is characteristic of (Ba-O) stretching mode, where the vibration frequency at 850 is characteristic of N-H bending mode, while the vibration frequency at 1376 cm^{-1} for O-H bending mode, the band at 1710cm^{-1} is responsible for the presence of C-O stretching mode. band at the range 2400- 2449 cm^{-1} is responsible for the presence of C=O (CO_2) stretching mode and the broad band peak appear from 2900-3500cm^{-1} is assigned to O-H stretching vibration caused by the presence of water molecules. These results are in good agreement with the one obtained by literature [22].

Figures 6a, b & c represent the STEM micrographs for Cu, Y and Ba complexes. The agglomerated nanoparticles are clearly observed with spherical shapes, the average grain size for the complexes are 5.0, 20.0 and 35.0 nm, respectively. After calcinations (Fig. 6d, e & f) the nanoparticles look more regular spheres with average grain size are 28.0, 20.0 and 45.0nm for CuO, Y_2O_3 and $BaCO_3$, Respectively.

UV-VIS spectrogram measured for all calcined NPs as shown in Fig. 7. The for Y_2O_3, $BaCO_3$ and CuO NPS are found to be 284.0 nm, 289.0 nm and 300.0 nm. These data are in the UV region as a sign for the nanometer scale of the produced powders. These results are in good agreement with that in the literature [20,23].

Conclusion

Copper oxide (CuO), yttrium oxide (Y_2O_3) and barium oxide ($BaCO_3$) nanoparticles were successfully prepared using green method, the neem fruit extract was used as a capping agent. The brown slurry was dried overnight at 80^oC, the calcination was carried out at 750^oC for CuO, $BaCO_3$ and Y_2O_3, respectively, for a period of 2 hours. the calcinations temperatures were selected on the basis of Thermal-Gravimetric Analysis (TGA)**.** X-ray Powder Diffraction analysis confirmed the monoclinic structure for CuO NPs, orthorhombic structure for $BaCO_3$ NPs and cubic structures for Y_2O_3 NPs. All the above-mentioned oxides data were matched with the ICDD standards. The crystallite size for the CuO, $BaCO_3$ and Y_2O_3 NPs were 29.9, 40.0 and

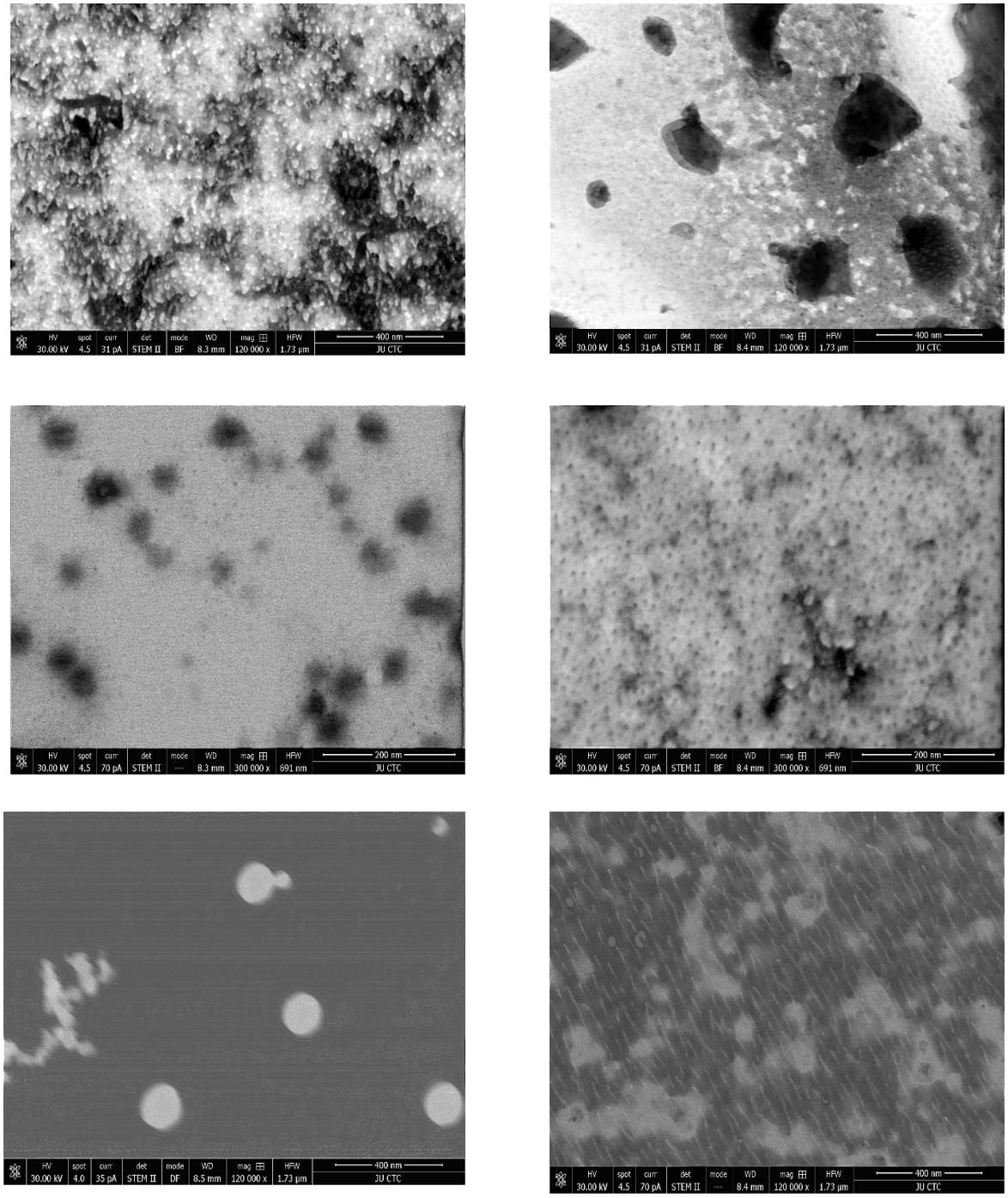

Fig. 6. STEM micrographs for (a) Cu-complex, (b) CuO NPs, (c) Y-complex, (d) Y_2O_3 NPs, (e) Ba-complex and (f) $BaCO_3$ NPs.

10.3 nm, respectively. UV-VIS spectroscopy showed that for the scanned suspended oxides were in the UV range which is an indication of the formation nano-sized materials, these results are in good agreement with the literature. STEM results showed agglomerated NPs with an average particle size of < 50 nm for all oxide samples. FTIR confirms the metal-oxide bands in the range 500-700nm^{-1}. Results of the current study are important for agricultural applications, industrial catalysis, petroleum industries, water splitting, production of ceramics and composite materials applications.

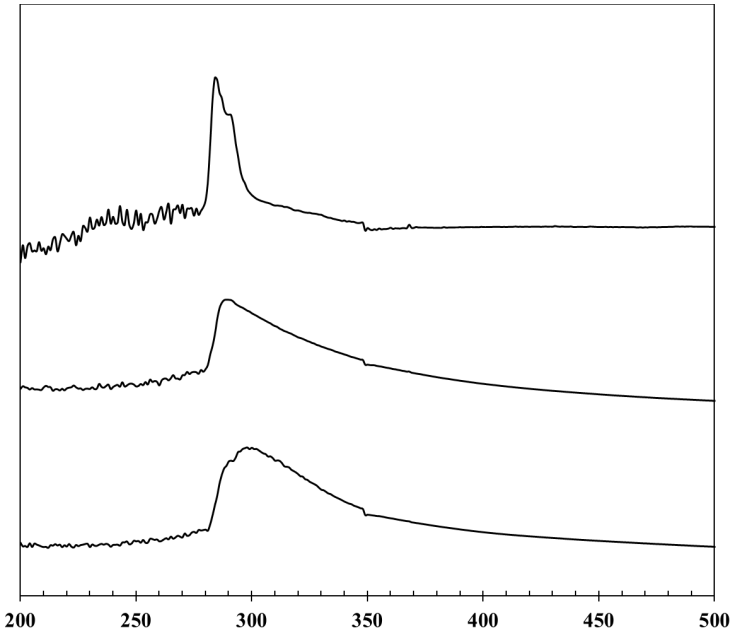

Fig. 7. UV-VIS spectrum for nanoparticles, (a) Y_2O_3, (b) CuO and (c) $BaCO_3$.

Acknowledgment

The authors would like to thank the Deanship of Academic Research and Quality Assurance at the University of Jordan for their financial support.

References

1. Shaban, S.A. Catalysis and nanotechnologies. *Egyptian Journal of Chemistry,* **55**(5), 453-473 (2012).

2. Ibrahim, A.H., Ismail, H.A.-., El-Desouki, D.S., Abdel-Azim, S.A. And Aboul-Gheit, N.A.K. Preparation of sulfated zirconia catalyst loaded by copper in 'nano-scale: Green application' to synthesis of biolubricant. *Egyptian Journal of Chemistry,* **61**(3), 503-516 (2018).

3. Ali, S.M., Galal, A., Atta, N.F. And Shammakh, Y. Toxic heavy metal ions removal from wastewater by nano-magnetite: Case study nile river water. *Egyptian Journal of Chemistry,* **60**(4), 601-612 (2017).

4. El-Alfy, E.A., Attya, M. And Shaaban, M.F. Treatment of cotton fabrics to inhibit bacterial effect of some microorganisms part I: Using separate nano antibacterial agents. *Egyptian Journal of Chemistry,* **58**(6), 671-680 (2015).

5. Nagajyothi, P. C. and Lee, K. D., Synthesis of plant-mediated silver nanoparticles using Dioscorea batatas rhizome extract and evaluation of their antimicrobial activities, *Journal of Nanomaterials*, **1**, 1-7 (2011).

6. Kharissova, O. V., Dias, H. R., Kharisov, B. I., Pérez, B. O. and Pérez, V. J., The greener synthesis of nanoparticles, *Trends in Biotechnology*, **31**(4), 240-248 (2013).

7. Zahran, M.K., Mohamed, A.A., Mohamed, F.M. And El-Rafie, M.H. Optimization of biological synthesis of silver nanoparticles by some yeast fungi. *Egyptian Journal of Chemistry,* **56**(1), 91-110. (2013).

8. Nadagouda, M. N., Hoag, G., Collins, J. and Varma, R. S., Green Synthesis of Au Nanostructures at Room Temperature Using Biodegradable Plant Surfactants, *Crystal Growth & Design*, **9**(11), 4979–4983 (2009).

9. Rajput, N., Methods of preparation of nanoparticles-a review, *Int. J. Advances in Eng. Techno.,* **7**(6), 1806(2015).

10. Nagajyothi, P. T., Sreekanth, V. M., Green Processes for Nanotechnology, *Springer International Publishing*, Switzerland, 99-117 (2015).

11. Makarov, V.V., Love, A. J., Sinitsyna, O.V., Makarova, S.S., Yaminsky, I.V., Taliansky, M.

E. and Kalinina, N. O., Green nanotechnologies: Synthesis of metal nanoparticles using plants, *Acta Naturae*, **6**(20), 35-44 (2014).

12. Fernández - García, M., Rodriguez, J. A., Metal oxide nanoparticles. *Encycl Inorg Bioinorg Chem*. Instituto de Catálisis y Petroleoquímica, CSIC, Madrid, Spain and Brookhaven National Laboratory, Upton, NY, USA (2011).

13. Gupta, S. C., Prasad, S., Tyagi, A. K., Kunnumakkara, A. B., and Aggarwal, B. B., Neem (Azadirachta indica): An indian traditional panacea with modern molecular basis, *Phytomedicine*, **34**, 14-20 (2017).

14. Thirumurugan, A., Aswitha, P., Kiruthika, C., Nagarajan, S., and Christy, A. N., Green synthesis of platinum nanoparticles using Azadirachta indica–An eco-friendly approach, *Mater. Lett.*, **170**, 175-178 (2016).

15. Oudhia, A., Kulkarni, P. and Sharma, S., Green synthesis of ZnO nanotubes for bioapplications, *Int. J. Advances in Eng. Techno.,* **IV/II**, 280-281 (2015).

16. Krishnasamyet, A., Sundaresan, M., and Velan, P., Rapid phytosynthesis of nano-sized titanium using leaf extract of Azadirachta indica, *Int. J. Chem Tech Res.,* **8**(4), 2047-2052 (2015).

17. Sankar, R., Rizwana, K., Shivashangari, K. S. and Ravikumar, V., Ultra-rapid photocatalytic activity of Azadirachta indica engineered colloidal titanium dioxide nanoparticles, *Appl. Nanoscience*, **5**(6), 731-736 (2015).

18. Sharma, R., Bisen, D. P., Shukla, U. and Sharma, B. G. X-ray diffraction: a powerful method of characterizing nanomaterials. *Recent Research in Science and Technology*, **4**(8)77-79 (2012).

19. Kannan, S. and Sundrarajan, M. Biosynthesis of yttrium oxide nanoparticles using Acalypha indica leaf extract, *Bull. Mater. Sci.***, 38**(4),945-950 **(**2015**).**

20. El-Trass, A., ElShamy, H., El-Mehasseb, I. and El-Kemary, M. CuO nanoparticles: Synthesis, characterization, optical properties and interaction with amino acids, *Appl.Surface Sci.,* **258**(7), 2997–3001 (2012).

21. Nasrollahzadeh, M., Sajadi, S. M., Rostami-Vartooni, A. and Hussin, S. M., Green synthesis of CuO nanoparticles using aqueous extract of Thymus vulgaris L. leaves and their catalytic performance for N-arylation of indoles and amines, *J. Colloid Interface Sci.*, **466**, 113-119 (2016).

22. Zeenath, A. and Amrina, M., Synthesis and Characterization of Barium Oxide Nanoparticles, *IOSR J. Appl. Phys.,* **3**, 76-80 (2017).

23. Avram, D., Cojocaru, B., Florea, M. and Tiseanu, C., Advances in luminescence of lanthanide doped Y_2O_3: case of S_6 sites. *Optical Mater. Express*, **6**(5), 1635-1643 (2016).

التصنيع الأخضر للحبيبات النانوية ($CuO, BaCO_3, Y_2O_3$) باستخدام الخلاصة المائية لثمرة النيم

عماد حمادنة[١]، هديل الحايك[١]، أحمد المبيضين[١]، أفنان أبو جابر[١]، رولى البقاعين[٢]، شروق السوطري[٢]، عمار الدجيلي[٣]

[١]قسم الكيمياء - كلية العلوم - الجامعة الأردنية - الرمز البريدي ١١٩٤٢ عمان - الأردن.
[٢]مركز الخلايا الجذعية - الجامعة الأردنية - الرمز البريدي ١١٩٤٢ عمان - الأردن.
[٣]مركز حمدي منكو للبحوث - الجامعة الأردنية - الرمز البريدي ١١٩٤٢ عمان - الأردن.

استخدمت الكيمياء الخضراء لتصنيع الحبيبات النانوية لأكسيد اليتيريوم (Y_2O_3) وكربونات الباريوم ($BaCO_3$) وأكسيد النحاس (CuO) بواسطة المستخلص المائي لثمرة النيم (أزيدراختا إنديكا) كعامل حماية. تم تسخين المعقدات المعدنية الناتجة عند درجة حرارة ٧٥٠ درجة مئوية. تم تشخيص الحبيبات النانوية الناتجة باستخدام جهاز حيود الأشعة السينية والمجهر الإلكتروني النافذ و الماسح و جهاز الأشعة تحت الحمراء و جهاز قياس الطيف الضوئي و جهاز التحليل الوزني الحراري. أكّدت تحاليل حيود الأشعة السينية بان الشكل البلوري لأكسيد النحاس النانوي مونوكلينيك، والشكل البلوري لكربونات الباريوم النانوية أورثورومبيك والشكل البلوري لأكسيد اليتيريوم النانوي مكعب وهي متوافقة مع المراجع االمعيارية. كان حجم بلورات CuO و$BaCO_3$ و Y_2O_3 هو٢٩,٩, ٤٩,٠ و ١٠,٣ نانومتر على التوالي. أظهر التحليل الطيفي للأشعة فوق البنفسجية أن قيمة طيف الامتصاص العظمى للأكاسيد المعلقة كانت في نطاق الأشعة فوق البنفسجية وهي مؤشر على تكوين مواد بحجم النانو. أظهرت نتائج المجهر الإلكتروني النافذ والماسح وجود جسيمات نانوية متكتلة بمتوسط حجمي قدره أقل من ٥٠ نانومتر لجميع عينات الأكاسيد الثلاث. أكدت نتائج الأشعة تحت الحمراء أن رابطة أكسيد الفلز موجودة في المدى ٥٠٠-٧٠٠ سم$^{-1}$.